Dual Polarization Operation of Nanostructure Arrays in the MIR Region

Ifeoma G. Mbomson[1], Ili F. Mohamad Ali Nasri[1], Richard M. De La Rue[1] and Nigel P. Johnson[1]

[1] *Optoelectronics Research Group, School of Engineering, University of Glasgow, Glasgow, G12 8LT, U.K.*

Abstract

In this paper, we report on arrays of asymmetric split H-shape (ASH) nanostructures tuned to produce two distinct resonances at wavelength that range from 3 µm to 7 µm. The electric-field of the incident wave has been both polarized parallel to the vertical asymmetric dipole arms and polarized across the 50 nm gap in the asymmetric horizontal bar. We have produced resonance quality factors as large as 26 in the MIR region.

Text

Metallic nanostructures have recently been applied to a wide range of situations because of their geometrical tunability - producing plasmonic resonances in various regions of the electromagnetic spectrum. In the MIR region, the characteristics of the plasmonic resonances from different MNs have been reported, for e.g., split-ring resonators[1-2], multiplexed cross resonators[3], and H-shaped nano-resonators[4]. The existence of various molecular bond resonances in the MIR region has attracted much research interest and promoted the application of metallic nanostructures for purposes such as bio-sensing[5-7]. In many cases, metallic nanostructures (MNs) exhibit a single characteristic plasmonic resonance peak operating in the MIR region

and a strongly polarization dependent response. The independent and single polarization operation metallic nanostructures that have been reported so far have typically produced Q-factor values in the range from 3.5 to 7[1-3,8]. A Q-factor of 13.9 was produced from the Fano resonance of an A-SRR structure[9]. The Q-factor values achieved reflect the material losses at frequencies in the MIR region[10-11]. A high resonance Q-factor is a desirable characteristic for sensors based on metallic nanostructures. In the past, different high sensitivity sensors with a low Q-factor have been developed in the MIR region[5-6]. Moderately high Q-factor values have been reported for excitation of normally incident light upon arrays of MNs in the visible, near infrared and microwave spectral regions[10-15]. Wang et al have demonstrated a coupled structure that combines a ring and a rod, Q-factor values, at visible wavelengths, as large as 100 are obtained in a simulation that includes realistic estimates of the Ohmic losses[15]. Researchers have produced structures with high Q-factor values in the MIR region by realising nanostructures with purely dielectric materials,[16-18] thereby escaping the Ohmic losses associated with metallic nanostructures. References[5,19] stated that most studies of surface-enhanced infrared spectroscopy used gold because it has been shown to produce strong enhancement with monolayer sensitivity. The characteristics of metallic nanostructures and usefulness have prompted a continuous optimization of the plasmonic resonance in MIR region. A Q-factor of 26 from both experiment and numerical simulation has been achieved in this work, by varying the array period of the asymmetric split H-shape nanostructure. Through experimental and numerical simulation, we have developed a metallic nanostructure that the resonance response dependent on dual polarization of light produced higher Q-factor than that reported in the MIR region [1-3, 8-9].

A close-packed periodic arrangement in an array of metallic nanostructures can produce the desirable combination of high peak reflectivity and strong resonance enhancement[14, 20]. Because of significant coupling between the individual ASH elements in an array, the density of the array nanostructure determines the peak reflectivity obtainable, while controlling peak broadening and the effective resonant spectral selectivity[14, 20-21]. The asymmetric feature of the ASH nanostructure was orthogonally designed in both x- and y-axes of the electric mode as shown in Fig. 1. The asymmetric nanostructures produce two distinct plasmonic resonance peaks that are strongly dependent on the dual polarization of the incident electromagnetic waves. By applying a sufficiently large periodic spacing in our dual-polarization dependent asymmetric H-shape nanostructure array, high Q-factors were achieved in the MIR region.

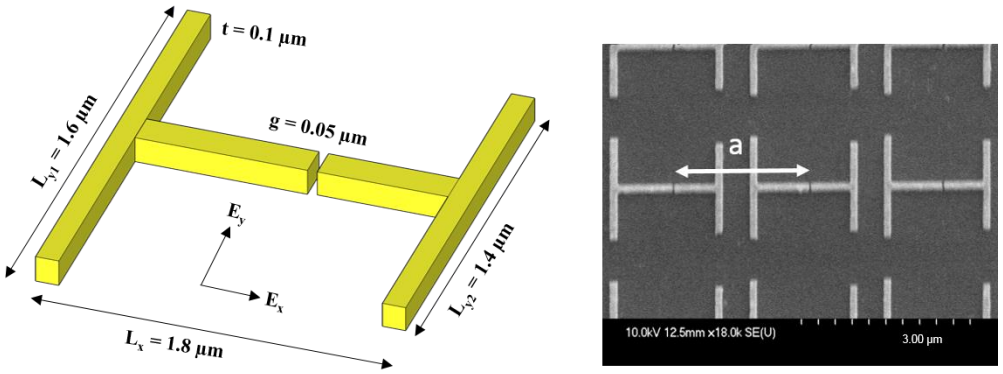

(a) (b)

FIG. 1. Schematic illustration of the asymmetric split H-shape metamaterial structure, where L_y , g, t and L_x denote the length in y-direction, gap, thickness and total length of the ASH structures along their x-direction, respectively. E_x and E_y denote the transverse electric mode in x- and y-axes of the design. (b) SEM image of asymmetric H-shape with array period **a**, of 2.6 μm.

The ASH nanostructure was formed with dipole strips having a width of 100 nm, as shown in Fig.1. The length dimensions of the horizontal asymmetrically located cross-bar sections, with a gap (*g*) in-between are 0.875 μm and 0.675 μm, respectively. The two sets of reflectance resonance peaks produced by the asymmetric structure provide a dual polarization response to the incident electromagnetic waves and their spectral positions were adjusted by varying the period of the array of the ASH nanostructure in both the x- and y-directions, as shown in Fig. 2. A dense array of ASH structures tends to produce plasmonic resonances with a higher reflectance magnitude. As a result of the high optical reflectivity from gold, the less dense design has lower reflectance. However, the resonance Q-factor is increased because of weaker coupling between the ASH elements in the sparser array.

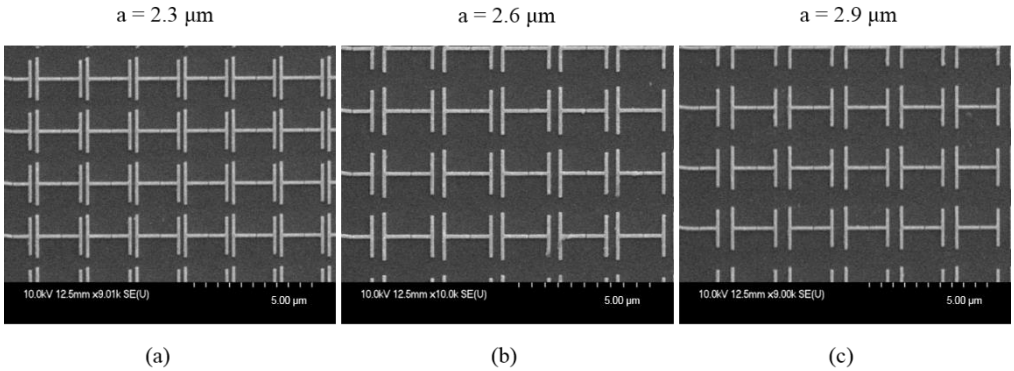

FIG. 2. SEM images of ASH with equal periodic array in a_{xy} axes for (a) a = 2.3 μm (b) a = 2.6 μm (c) a = 2.9 μm.

Because of stronger inter-element coupling, the high value of the resonant reflectance from a denser design may lead to significantly broader resonance peaks. Figures 2(a) to (c) show scanning electron microscopy (SEM) images of parts of ASH arrays with equal ASH dimensions in all cases, but different periods of 2.3 μm, 2.6 μm and 2.9 μm respectively, along both the x- and y-axes. The corresponding spacing between

the adjacent ASHs are 0.5 μm, 0.8 μm and 1.1 μm, respectively. The image for the 2 μm period is not included as the fabricated structures merged. The fabrication process for the ASH nanostructures followed a similar procedure to that described in reference[22]. The strip width for both the asymmetric dipoles and the bars of the ASH structures was 100 nm on a 960 μm thick fused silica substrate. Numerical simulations were performed using software from Lumerical. The FDTD simulation region for the ASH nanostructure applied to the x- and y-axes used periodicity conditions, with array periods of 2.3 μm, 2.6 μm and 2.9 μm as shown with the SEM images. Perfectly matched layers (PML) were used along the z-axis for near total absorption of the normally incident electromagnetic waves for interaction with the array of ASH structures.

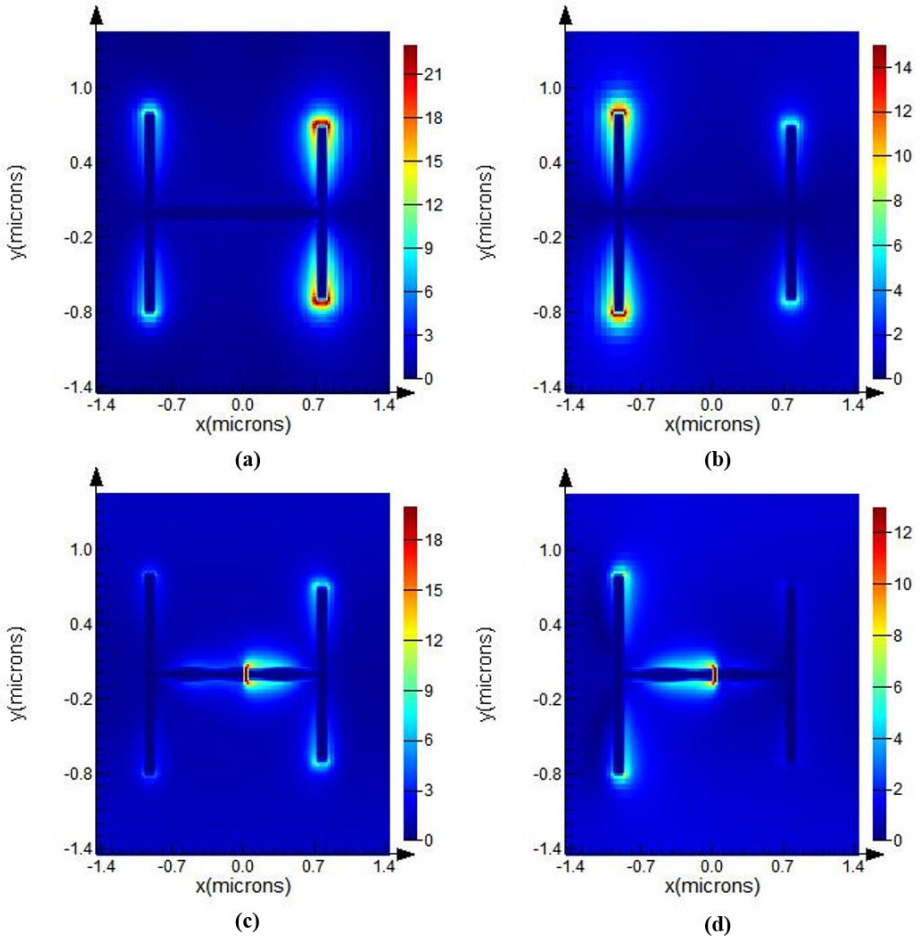

FIG. 3. Electric field distribution plots in a single unit-cell of the ASH from the FDTD simulations, at different peak wavelengths: (a) peak resonance at approximately 4.2 μm for E_y polarizations and (b) peak resonance at approximately 5.2 μm for E_y polarizations (c) resonant at approximately 4.2 μm and (d) 5.03 μm for the E_x polarizations

The electric field plots of the ASH structure at the wavelengths at approximately 4.2 μm, 5.2 μm and 5.03 μm for both polarizations indicate excitation of the resonant mode which induces an oscillation of the EM wave in the metallic structure as shown in Fig. 3. Concentration of the field strength at the end of each arms of the ASH structure in this scenario describe the electric distribution for the E_y and E_x polarizations of EM wave at the plasmonic resonance peaks.

A Fourier transform infrared (FTIR) spectrometer coupled to a Nicolet Continuum microscope was used to measure the reflectance spectra of the fabricated ASH arrays,

as shown in Fig. 4. In the reflectance spectra, the smaller and larger metallic dipole resonances produce reflection peaks at shorter and longer wavelengths respectively. These resonant reflectance peaks also produced by the horizontal asymmetric cross bars of the ASH.

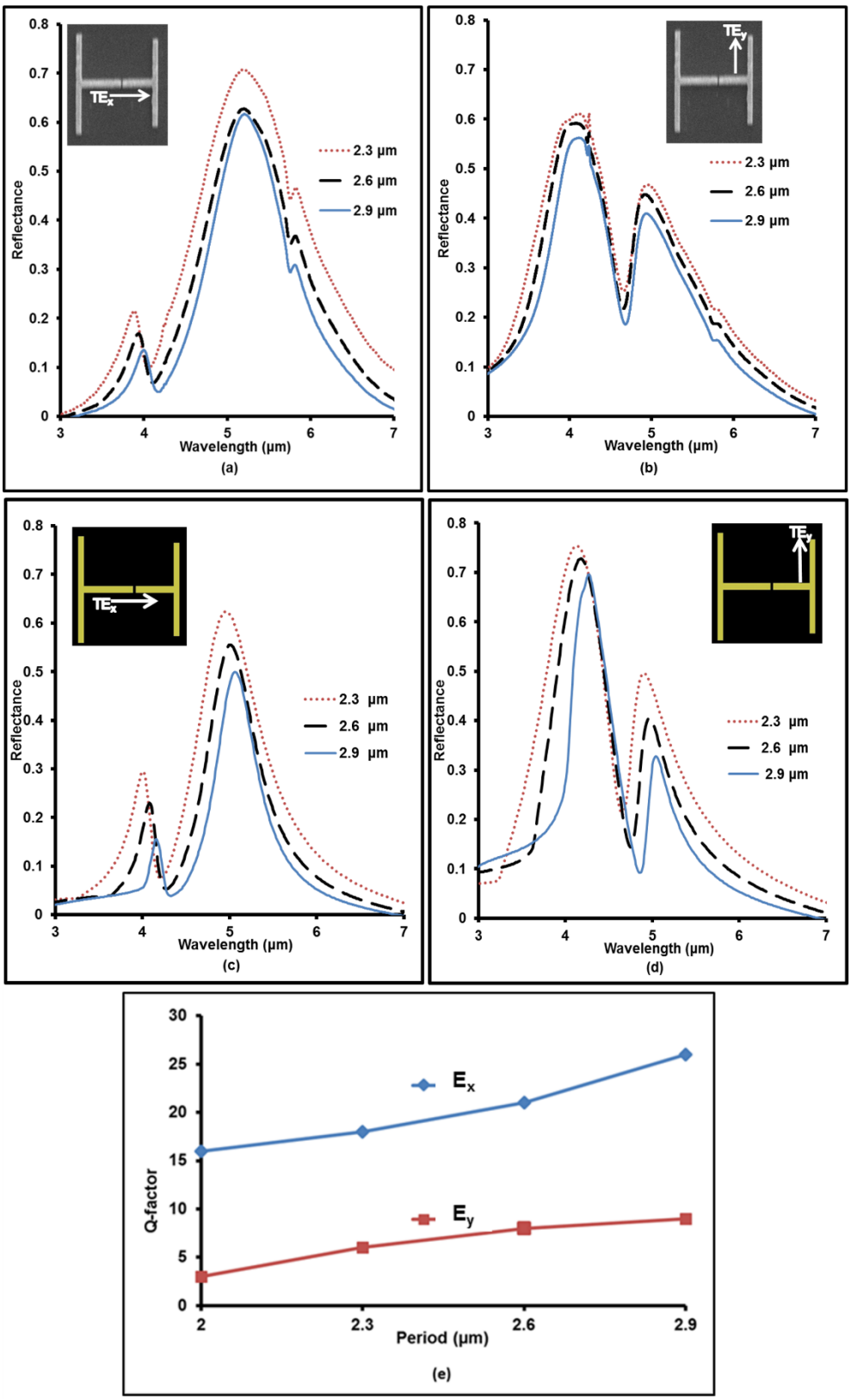

FIG. 4. Inset SEM image of ASH on the plots for the reflectance spectra peaks from the FTIR measurements. The two distinct resonance peaks correspond to the small and large arms of the ASH produced when the electric mode is (a) across the gap along the x-axis (b) along the y-axis. The ripples

at approximately 4.2 μm and 5.8 μm are from atmospheric CO_2 and the C=O bond vibrational resonance of PMMA, respectively. Again, the insets show schematic images of the ASH structures on the plots for the reflectance spectral peaks obtained from numerical simulation with the electric field polarized: (c) across the gap along the x-axis and (d) along the y-axis. (e) Comparison graph of Q-factor for E_x and E_y polarization of the incident light electromagnetic waves.

The resultant experimental reflectance spectra are shown in Figs. 4(a) and (b), with resonance peaks obtained at approximately the same positions as the simulated reflectance spectra shown in Figs. 4(c) to (d). The effect on the resonance peaks of varying the periodic spacing was similar for simulation and experiment. The figures show the reflected light from the sample surface normalized with respect to the amount of electromagnetic radiation incident on the array. The same calculation also gives transmittance of the array. Conservation implies that the remaining energy contribution is due to absorption. The figures demonstrate that the design operates in dual polarization mode - but also that the reflectance magnitude is different for the two orthogonal polarisations. The calculated Q-factor values for both the E_x and E_y polarizations are based on the plasmonic resonance at the shorter wavelengths (~ 4.2 μm) of the plots in Figs. 4. The plots in Figs. 4 show reductions in the amplitude of the resonant reflection peaks, as the array period and inter-element spacing increase, as observed in the numerical simulations. In comparison with this paper, Cao et al[23] have demonstrated a transmission resonance Q-factor of 227 at 0.5 THz (~ 600 μm) in a slightly asymmetric split-ring structure, with progressively smaller peak magnitudes. Figure 4(e) shows the simulation results for Q-factors in dual polarization operation for periods in the range from 2 μm to 2.9 μm. In the E_y polarization, for a high Q-factor, a period value of 3.2 μm which is greater than twice the length of the ASH structure dipole arms was applied[24]. For Ex polarization, the array period is approximately four times the length of the asymmetric arms of the

structure. Figures 4 explicitly show the two distinct resonance peaks produced when our asymmetric nanostructure was excited with dual polarized incident electromagnetic waves.

In conclusion, enhanced surface plasmonic resonance has been investigated by several groups of researchers, because of the wide range of applications such as molecular sensors. Environmental and biochemical sensor applications require high Q-factors to maximise sensitivity. We report ASH nanostructure arrays that may be excited in dual polarization to produce a *Q*-factor value of 26 in the x-polarization, a value that is twice the previously reported value[9] for plasmonic sensors in the MIR region. This performance was achieved by applying a suitable array period value in our design and was confirmed for the resonance peaks of the reflectance spectra in both simulation and experiment. The double resonance peaks in the reflectance spectra produced by our ASH structure arrays can enhance the sensitivity for two different and orthogonal polarisations of incident electromagnetic waves in the MIR, enabling dual polarisation operation.

Acknowledgement

This research work was funded by Majlis Amanah Rakyat (MARA) Malaysia and J.J Mbomson Education Foundation. The authors would also like to acknowledge the facilities and staff of the James Watt Nanofabrication Centre for their support during fabrication of the structures.

References

[1]B. Lahiri, A. Z. Khokhar, R. M. De La Rue, S. G. McMeekin, and N. P.Johnson, Opt. Express 17(2), 1107 (2009).

[2]W. Yue, Z. Wang, J. Whittaker, F. Schedin, Z. Wu, and J. Han, Nanotechnology 27, 055303 (2016).

[3]W. Ma, Y. Wen, and X. Yu, Opt. Express 21(25), 30725 (2013).

[4]Z. H. Jiang, S. Yun, F. Toor, D. H. Werner, and T. S. Mayer, ACS Nano, 5 (6), 4641 (2011).

[5]I. M. Pryce, Y. A. Kelaita, K. Aydin, and H. A. Atwater, ACS Nano 5, 8167 (2011).

[6]B. Lahiri, S. G. McMeekin, R. M. De La Rue, and N. P. Johnson, Opt. express 21, 9343 (2013).

[7]I. G. Mbomson, S. Tabor, B. Lahiri, G. Sharp, S. G. McMeekin, R. M. De La Rue, and N. P. Johnson, Biomed Opt Express 8(1), 395 (2017).

[8]G. J. Sharp, H. Vilhena, B. Lahiri, S. G. McMeekin, R. M. De La Rue, and N. P. Johnson, Appl. Phys. Lett. 108(25), 251105 (2016).

[9]J. Chae, B. Lahiri, and A. Centrone, ACS Photonics 3, 1 (2016).

[10]V. A. Fedotov, M. Rose, 1 S. L. Prosvirnin, N. Papasimakis, and N. I. Zheludev, PhysRevLett, 99, 147401(2007).

[11]K. Aydin, I. M. Pryce, and H. A. Atwater, Opt. express 18, 13407 (2010).

[12]I. Al-Naib, E. Hebestreit, C. Rockstuhl, F. Lederer, D. Christodoulides, T. Ozaki, and R. Morandotti, Phys. Rev. Lett. 112, 183903 (2014).

[13]Y. Yang, I. I. Kravchenko, D. P. Briggs, and J. Valentine, Nature Communications, 6753 (2014).

[14]J. Shu, W. Gao, K. Reichel, D. Nickel, J. Dominguez, I. Brener, D. M. Mittleman, and Q. Xu, Opt. Soc. 22(4), 3748 (2014).

[15] J. Wang, B. Yuan, C. Fan, J. He, P. Ding, Q. Xue, and E. Liang, Opt. Express 21, 21(2013).

[16]J. Zhang, K. F. MacDonald, and N. I. Zheludev, Opt. Soc. Am. 39, 4883 (2014).

[17]C. Wu, N. Arju, G. Kelp, J. A. Fan, J. Dominguez, E. Gonzales, E. Tutuc, I. Brener, and G. Shvets, Nature Communications 5, 3892 (2014).

[18]Y. Yang, I. I. Kravchenko, D. P. Briggs, and J. Valentine, Nature Communications 5, 6753 (2014).

[19]M. Abb, Y. Wang, N. Papasimakis, C. H. de Groot, and O. L. Muskens, Nano Lett. 14, 346(2013).

[20]R. Singh, C. Rockstuhl, and W. Zhang, Appl. Phys. Lett. 97(24), 241108 (2010).

[21]M. Abb, Y. Wang, N. Papasimakis, C. H. de Groot, and O. L. Muskens, Nano Letter 14, 346 (2014).

[22]I. G. Mbomson, S. G. McMeekin, R. M. De La Rue, and N. P. Johnson, Proc. SPIE USA 9340, 93400G (2015).

[23]W. Cao, R. Singh, I. A. I Al-Naib, M. He, A. J. Taylor, and W. Zhang, Opt. Letters 37, 16 (2012).

[24]I. F. Mohamad Ali Nasri, I. G. Mbomson, R. M. De La Rue, and N. P. Johnson, Proc. SPIE Europe 9883, 98831N (2016).